Swift heavy ions induced modifications in structural and electrical properties of polyaniline

R. C. Ramola[1,*], Subhash Chandra[1], J. M. S. Rana[1], Raksha Sharma[2], S. Annapoorni[2], R. G. Sonkawade[3], Fouran Singh[3] and D. K. Avasthi[3]

[1]Department of Physics, HNB Garhwal University, Badshahi Thaul Campus, Tehri Garhwal 249 199, India
[2]Department of Physics and Astrophysics, University of Delhi, Delhi 110 007, India
[3]Inter University Accelerator Centre, Aruna Asaf Ali Marg, New Delhi 110 067, India

The ion fluences range from 5×10^{10} to 1×10^{12} ions/cm^2 irradiation effects of 50 MeV Li^{3+} and 90 MeV C^{6+} ion beams on free-standing polyaniline (PANI) films have been investigated. The X-ray diffraction study shows an increase in crystalline nature of the PANI film with increasing fluence, followed by a decrease beyond the critical ion fluence. I–V characteristics reveal increased conductivity in the irradiated films. Scanning electron microscopy shows the formation of clusters and craters at higher fluences.

Keywords: Electrical properties, polyaniline, scanning electron microscopy, swift heavy ions, X-ray diffraction.

CONJUGATED polymers, having delocalized π electrons, constitute an important class of materials due to their properties such as high electrical conductivity and large nonlinear optical responses. One of these polymers, particularly polyaniline (PANI) has been the centre of considerable scientific interest in recent years. PANI is a favourable polymer to work with because of its chemical stability[1], ease of synthesis[2,3] and variability of its conductivity through doping[4]. PANI displays a wide spectrum of applications such as conductive surface[5], electrochromic devices[6], piezoelectric devices[7], photoconductors[8] and microactuators[9]. The flexibility of PANI coupled with the high conductivity of doped PANI has made it a good material for electromagnetic shielding. PANI has been modified by number of methods like plasma processing, laser ablation[10], scanning probe microscopy[11] and ion beam treatment[12] resulting in molecular arrangement, crystallinity, cross-linking and scission of polymer chains[13], hardness changes[14,15], improved wear resistance[16], increased electrical conductivity[17] and change of optical properties.

Irradiation of materials by swift heavy ions (SHI) has attracted much attention as it induces large property variations. Ion beams have induced significant changes in structural, electrical and optical properties of conjugated polymers[18–21] and was shown to form electrically conducting nanowires along the ion track[22,23]. During irradiation of polymers by high-energy ions, their energy is transferred into the target material by electronic energy loss. This energy transfer leads to the formation of reactive species like radicals, gases and defects in the form of unsaturation, scissoring and cross-linking of the polymers. Recently a transition from insulating to carbonized conducting state was observed in PANI by high energy C^{2+}, F^{2+} and Cl^{2+} ions[24]. The I–V characteristics of PANI irradiated with Ar ions from a dense plasma focus (DPF) showed a diode-like behaviour[25]. Polymer dissociation and selective depletion of volatile species by ion bombardment may lead to new useful composites[26]. Changes of crystallinity of polymers by ion irradiation have been reported in the literature[27–34]. However, changes in crystallinity under high-energy ion irradiation in conjugated polymers have not been studied in detail till now. Our interest is to quantify changes induced by SHI on conductivity and crystallinity. In this communication, the effects of 50 MeV Li^{3+} and 90 MeV C^{6+} ions on structural, electrical and morphological properties of the free-standing PANI films are reported.

PANI films of thickness ~100 μm were synthesized by a standard procedure[35]. For the polymerization of PANI, the aniline monomer (0.1 M) was dissolved in HCl (1 M) at ice temperature and stirred for 30 min or till the droplets of the monomer disappear. The ammonium persulphate (0.2 M) was then added dropwise to the solution at the same temperature for about 90 min. The resulting solution was filtered and washed with double distilled water and alcohol. This solution was again filtered and treated with the Soxhlet assembly for the removal of oligomers or any impurity present in the solution. The solution was then dried and washed with ammonia for undoping; then again it was filtered and dried at 40°C. The resulting brown colour powder was dissolved in *N*-methyl-2-pyrrolidone (NMP) and stirred for 24 h. The solution was again filtered and the filtrate was kept in a tray at 60°C. A smooth film was obtained, which was doped by HCl.

The free standing films of 1 sq. cm were irradiated by 50 MeV Li^{3+} and 90 MeV C^{6+} ion beams under high vacuum in a 15 UD Pelletron accelerator. The ion beam fluence varied from 5×10^{10} to 3×10^{12} ions/cm^2 with a beam current of 3 pnA for Li^{3+} and 1.5 pnA for C^{6+} ions. The ion ranges exceeded the film thickness. To expose the whole area, the beam was scanned by an electromagnetic scanner. The irradiated PANI films were characterized by X-ray diffraction (XRD) in Bragg-Brentano geometry (Philips X-ray Diffractometer) with Cu-Kα radiation (=1.5918 Å). Electrical properties were measured using a conventional four probe method at room temperature. The current was varied using a Keithley meter and the voltage was measured using a low-voltage power

*For correspondence. (e-mail: rcramola@gmail.com)

Table 1. The SRIM 2003 calculated S_e, S_n and range for Li^{3+} and C^{6+} ions in polyaniline films

Target	Ion beam	Energy (MeV)	S_e (eV/Å)	S_n (eV/Å)	Range (μm)
Polyaniline	Lithium	50	5.836E + 00	3.288E–03	485.23
	Carbon	90	2.229E + 01	1.191E–02	240.18

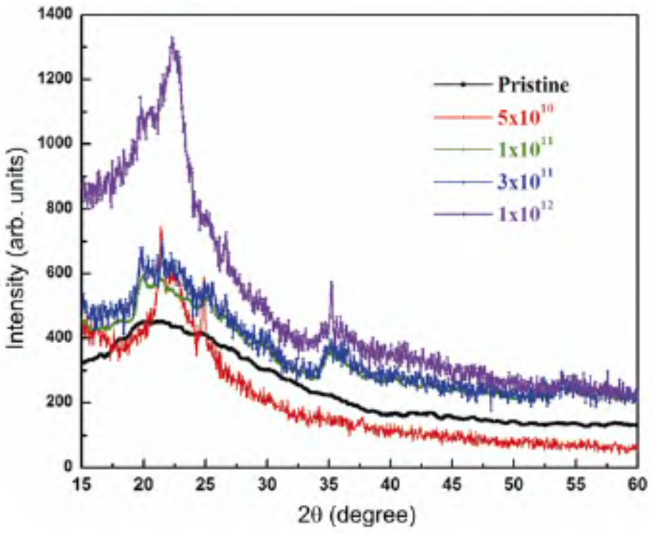

Figure 1. X-ray diffraction pattern of pristine and 50 MeV Li^{3+} ions beam irradiated polyaniline films.

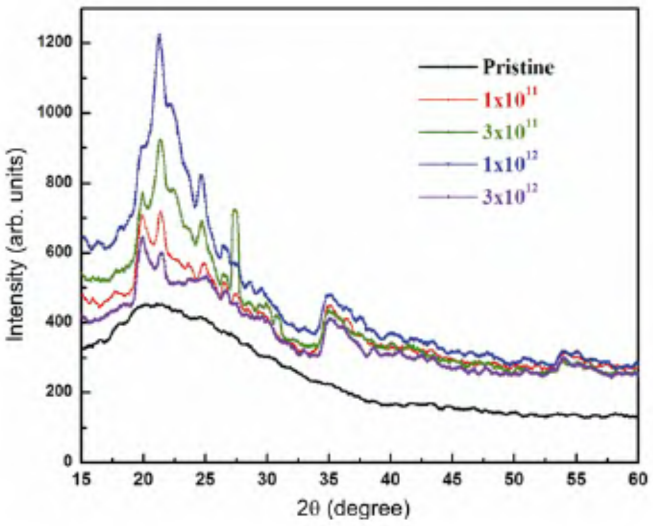

Figure 2. X-ray diffraction pattern of pristine and 90 MeV C^{6+} ions beam irradiated polyaniline films.

supply. The point contacts were made of gold, thermally evaporated on the polymer film. A JEOL JSM 840 scanning electron microscope (SEM) was used to investigate the surface modification induced in the film by ion-irradiation.

It is well known that most of the energy loss of SHI is electronic in nature. The nuclear energy loss is low and almost negligible throughout the film. The electronic stopping power of PANI film as calculated by the stopping range of ions in matter (SRIM)[36] programme is 5.84 eV/Å for Li^{3+} and 22.3 eV/Å for C^{6+} ions. The range of ions in the PANI film was calculated by the SRIM programme. The projected ranges for the Li^{3+} and C^{6+} ions in PANI films are 485 μm and 240 μm respectively. The projected range is much higher than the thickness of the polymer film and thus allows ions to pass through the film. The SRIM calculations for both of the ions are given in Table 1.

The XRD of PANI films before and after the irradiation by 50 MeV Li^{3+} and 90 MeV C^{6+} ions is presented in Figures 1 and 2 respectively. The pristine PANI film shows semicrystalline behaviour. A significant increase in the degree of crystallinity (DOC) was observed after irradiation.

The DOC is determined by integrating over the XRD peak. The normalized integral intensity gives volume fraction crystallinity (Φ_c). The determination of DOC implies using the two-phase model[37]. Determination of Φ_c, from the XRD pattern under the two-phase assumption, involves separation of diffraction pattern into three parts: (i) crystalline, (ii) amorphous and (iii) Compton background (incoherent scattering). The diffracted intensity is proportional to the sum of these contributions. The Φ_c is given by the ratio of the integral of crystalline diffraction intensity over the total coherent scattering, after subtracting the incoherent scattering. Table 2 shows the DOC for lithium and carbon irradiated films. The DOC was found to increase proportionally with fluence up to a dose of 1×10^{12} ions/cm^2 beyond which it decreases. The increase in DOC of polymer films by SHI irradiation[38] could be attributed to reorganization of molecular bonds, related to multiple excitation and ionization events on an extremely short space and time scale. In SHI irradiation, the density of the polymer increases making the polymer more compact, which may have produced closely packed regions by chain folding, cross-linking of polymer chains or by the formation of single or multiple helices[39], which produces more crystalline regions in the polymer films resulting in an increase in DOC[40]. The density of these modified zones, having crystalline structures, increases with the increase in ion fluence. However, the polymer is carbonized at higher fluence due to overlapping of damaged zones, resulting in the decrease in DOC. The broadening of peaks in Figures 1 and 2 with increase in fluence suggests a change in the crystallite size on irradiation. The values of crystallite size, calculated using Sherrer's equation[41], are given in Table 3. The crystallite size of

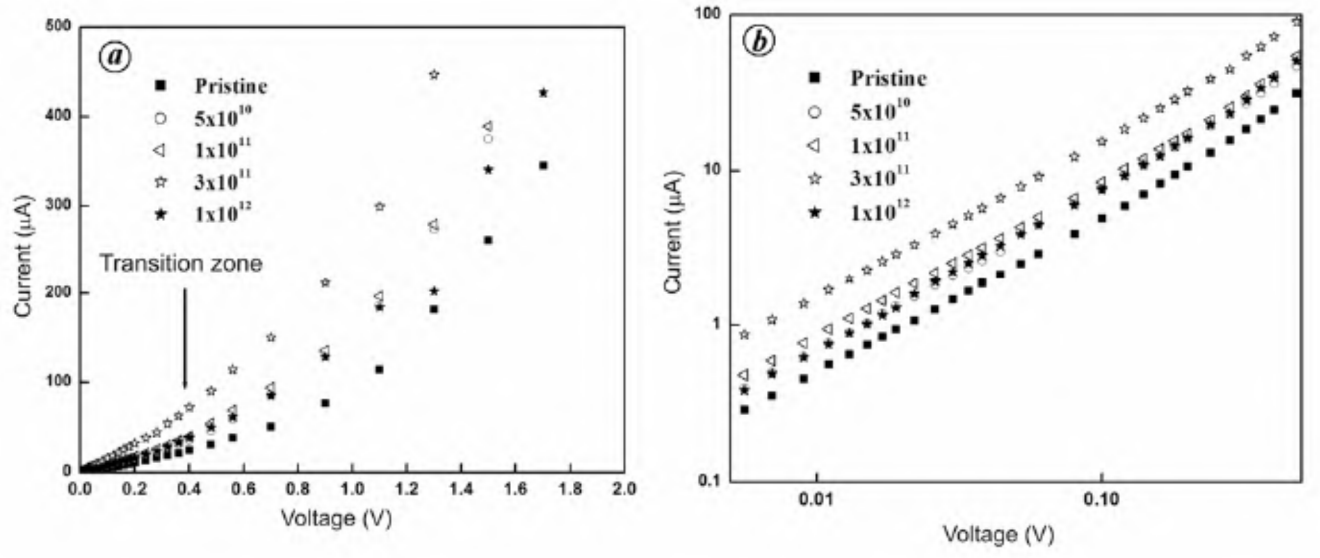

Figure 3. The I–V characteristic of polyaniline films: (***a***) Normal and (***b***) Log: log plot of I–V characteristics of polyaniline films for pristine and irradiated with 50 MeV Li^{3+} ions having fluences of 5×10^{10}, 1×10^{11}, 3×10^{11} and 1×10^{12} ions/cm^2.

Table 2. Degree of crystallinity of polyaniline films irradiated with 50 MeV Li^{3+} and 90 MeV C^{6+} ions

	Degree of crystallinity (%)	
Fluence (ions/cm^2)	50 MeV Li^{+3}	90 MeV C^{+6}
Pristine	30.2	30.2
5×10^{10}	32.8	–
1×10^{11}	43.7	37.4
3×10^{11}	43.7	39.4
1×10^{12}	52.7	46.3
3×10^{12}	–	33.7

Table 3. Crystallite sizes of Li^{3+} and C^{6+} irradiated polyaniline films

	Crystallite size (nm)	
Fluence (ions/cm^2)	50 MeV Li^{3+}	90 MeV C^{6+}
Pristine	14.2	14.3
5×10^{10}	12.6	–
1×10^{11}	10.9	15.2
3×10^{11}	9.8	13.1
1×10^{12}	8.7	11.3
3×10^{12}	–	10.4

the film was found to decrease with ion fluence[42]. The reduction in crystallite size is attributed to strain-induced fragmentation of grains. As fluence increases, the energy transferred by the ions to the electronic subsystem will increase, which results in further decrease in grain size. There was an average decrease in crystallite size of the order of 30.9% for Li^{3+} ions and 31.6% for C^{6+} ions with increase in fluence from 5×10^{10} to 1×10^{12} ions/cm^2 and 1×10^{11} to 3×10^{12} ions/cm^2 respectively. The electronic energy loss for 50 MeV Li^{3+} and 90 MeV C^{6+} ions in PANI films is 5.84 eV/Å and 22.3 eV/Å respectively, as estimated by SRIM.

The I–V characteristics of Li^{+3} and C^{+6} ion beams irradiated PANI films are shown in Figures 3 and 4 respectively. A nonlinear behaviour was observed. It is clear from log plots (Figures 3 *b* and 4 *b*) that the characteristics follow two power-law regions with different exponents. The power-law relationship can be expressed as $J = kV^n$, where k is a constant and n the exponent determined by slope of the curve. At low voltages, the current is proportional to the electric field. This corresponds to an Ohmic regime (exponent $n \sim 1$), which extends almost up to 1 volt (Figures 3 *b* and 4 *b*). With increasing bias voltage, the curve tends towards space charge limited conduction (SCLC) with $n > 2$, which is highly influenced by the presence of traps[43]. The power n depends upon the type of trap distribution, viz. single level traps, exponential distribution or Gaussian distribution, etc. in the energy space. It is observed that the transition voltage from the Ohmic regime to the space charge limited regime (V) increases slightly with increasing fluence. This implies that the background free charge carrier density increases slightly with increasing ion fluence[31]. This trend is observed in both cases; carbon and lithium irradiation. An exception is observed in the film irradiated with carbon at a fluence of 3×10^{12} ions/cm^2, where V was reduced. The reduction in V is due to lower number of free charge carrier density for highest fluence, which can be explained by the degree of order induced in the film by irradiation.

The XRD studies of PANI films show that they consist of nm sized (8–17 nm) crystallite zones surrounded by amorphous material. The charge transport takes place via

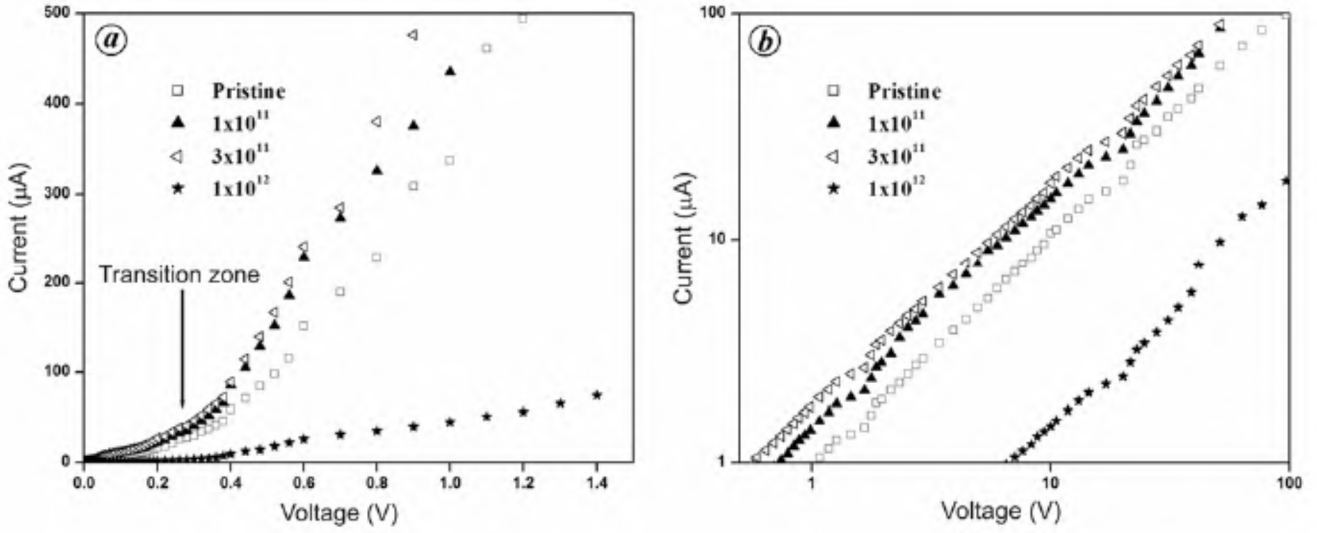

Figure 4. The I–V characteristic of polyaniline films: (***a***) Normal and (***b***) Log: log plot of I–V characteristics of polyaniline films for pristine and irradiated with 90 MeV C^{6+} ions having fluences of 1×10^{11}, 3×10^{11}, 1×10^{12} and 3×10^{12} ions/cm^2.

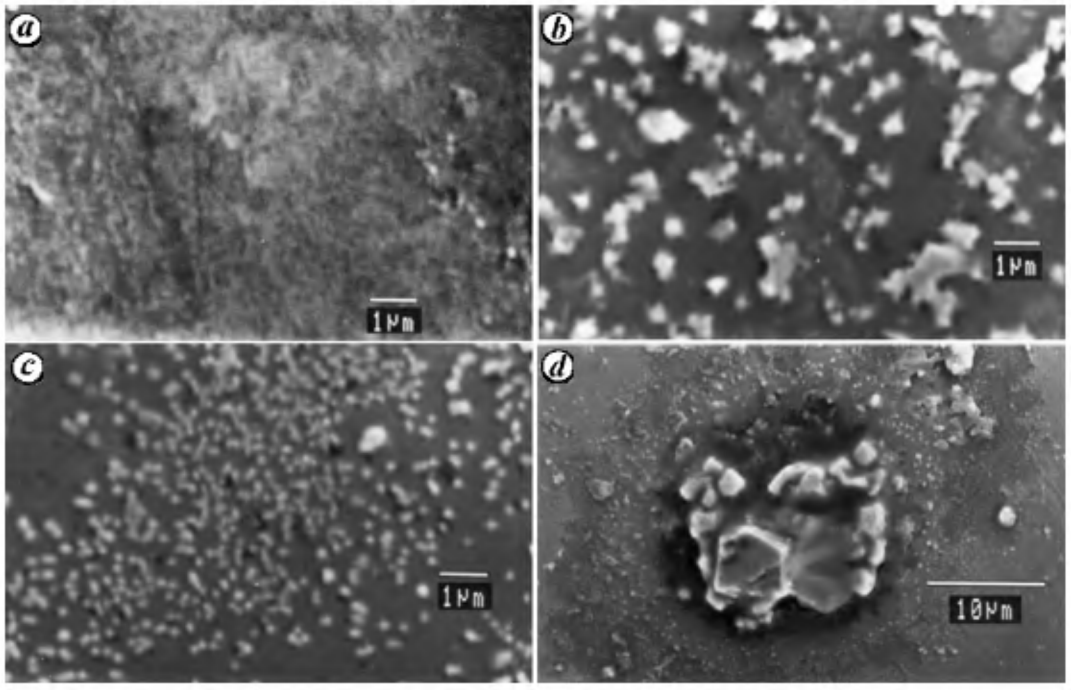

Figure 5. Scanning electron microscopy (SEM) of polyaniline films for (***a***) unexposed and exposed with 50 MeV Li^{3+} ions of the fluences (***b***) 5×10^{10}, (***c***) 1×10^{11} and (***d***) 1×10^{12} ions/cm^2.

two contributions: (i) metallic conduction through a crystallite core and (ii) thermally activated tunneling (hopping) through an amorphous barrier. The macroscopic conductivity of the film can be determined by measuring charge transport through amorphous barrier. An amorphous phase of PANI can exist in various conformations like 'coil', 'expanded coil' or 'rod-like' entities. The re-crystallization induced by irradiation leads to chain alignment and increases the degree of order in the film. Thus conductivity can be looked upon as metallic conduction interrupted by small barriers. Conduction electrons are three dimensionally delocalized in the 'crystalline' ordered regions and diffuse along the electronically isolated chains through disordered regions, where electrons are localized. The higher the crystallite ordered regions in the material, higher the conductivity expected. With the increasing fluence, the DOC increases (Table 2) and hence the density of free charge carriers increases in

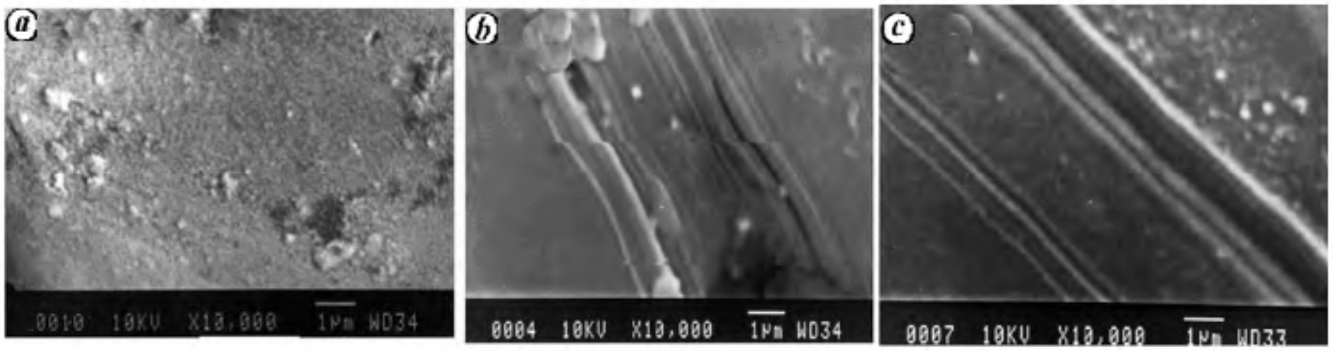

Figure 6. Scanning electron microscopy (SEM) of polyaniline films for exposed with 90 MeV C^{6+} ion of the fluences (*a*) 5×10^{10}, (*b*) 1×10^{11} and (*c*) 1×10^{12} ions/cm^2.

the form of defects, polarons and bipolarons. Thus a slight increase in transition voltage (V) with increasing fluence is observed (except for highest fluence, where DOC decreases due to overlapping of damaged zones).

The surface morphology of pristine and irradiated films was analysed by SEM. Figure 5 shows SEM images of PANI films before and after irradiation with Li^{3+} ions. The film irradiated with a fluence of 5×10^{10} ions/cm^2 shows formation of random shape clusters having dimensions of 0.1–3 μm (Figure 5 *b*). On increasing the fluence to 1×10^{11} ions/cm^2, cylindrical shape structures with longer and shorter axis of 500 nm micrometre and 100 nm respectively are observed (Figure 5 *c*). No such structures were observed for samples, irradiated with a fluence of 1×10^{12} ions/cm^2, though craters (~15 μm) were observed in some places (Figure 5 *d*). The formation of clusters may be due to large amount of electronic energy deposited in the films by Li ions. The SEM images of PANI film irradiated with 90 MeV carbon ions are shown in Figure 6. The formation of clusters of granular structures at low fluence (5×10^{10} ions/cm^2) can be attributed to energy loss-induced collision cascades, which take place near the surface and are responsible for the displaced atoms forming clusters (Figure 6 *a*). As the fluence increases (1×10^{11} ions/cm^2), electronic energy loss induced sputtering effects remove the surface layers and subsequent reduction in cluster size is observed (Figure 6 *b*). At higher fluence (3×10^{11} ions/cm^2), the higher sputtering rate contributes to formation of craters.

The crystalline nature of free-standing PANI films was found to increase with increasing ion fluence, followed by a decrease beyond the critical fluence. With increasing ion fluence, the DOC increases, whereas the crystallite size decreases. After irradiation, a slight variation was also observed in the resistivity of the film, which is due to the formation of polaron and bipolaron. SEM study shows that the ion beam irradiation leads to formation of clusters and craters in PANI films.

1. Hobaica, S. C., Stability of polyaniline in air and acidic water. *J. Polym. Sci. B: Polym. Phys.*, 2003, **41**, 807–822.
2. MacDiarmid, A. G., Chiang, J. C., Richte, A. F. and Epstein, A. J., Polyaniline: a new concept in conducting polymers. *Synth. Met.*, 1987, **18**, 285–290.
3. MacDiarmid, A. G. and Epstein, A. J., The concept of secondary doping as applied to polyaniline. *Synth. Met.*, 1994, **65**, 103–116.
4. Lee, K., Heeger, A. J. and Cao, Y., Reflectance of polyaniline protonated with camphor sulfonic acid: disordered metal on the metal–insulator boundary. *Phys. Rev. B*, 1993, **48**, 14884–14891.
5. Li, Z. F. and Ruckenstein, E., Strong adhesion and smooth conductive surface via graft polymerization of aniline on a modified glass fiber surface. *J. Colloid Interface Sci.*, 2002, **251**, 343–349.
6. Yang, C. H., Chih, Y. K., Chang, Wu, W. C. and Cheng, C. H., Molecular assembly engineering of self-doped polyaniline film for application in electrochromic devices. *Electrochem. Solid-State Lett.*, 2006, **9**, C5–C8.
7. Trivedi, D., Polyanilines. *Handbook of Organic Conductive Molecules and Polymers* (ed. Nalwa, H. S.), Wiley, New York, 1996, vol. 2, p. 505.
8. Chandrasekhar, P., *Conducting Polymers, Fundamentals and Application*, Kluwer Academic Publishers, Boston, 1999, p. 143.
9. Otero, T., Artificial muscles, electrodissolution and redox processes in conducting polymers. In *Handbook of Organic Conductive Molecules and Polymers* (ed. Nalwa, H. S.), Wiley, New York, 1997, vol. 4, p. 517.
10. Lippert, T., Raimondi, F., Wambach, J., Wei, J. and Wokaum, A., Surface modification and structuring of electrical conducting and isolating polyaniline films. *Appl. Phys. A*, 1999, **69**, S291–S293.
11. Ono, T., Yoshida, S. and Esashi, M., Electrical modification of a conductive polymer using a scanning probe microscope. *Nanotechnology*, 2003, **14**, 1051–1054.
12. Davenas, J., Xu, X. L., Boiteux, G. and Sage, D., Relation between structure and electronic properties of ion irradiated polymers. *Nucl. Instrum. Meth. Phys. Res. B*, 1989, **39**, 754–763.
13. Wintersgill, M. C., Ion implantation in polymers. *Nucl. Instrum. Meth. Phys. Res. B*, 1984, **1**, 595–598.
14. Swain, M. V., Perry, A. J., Treglio, J. R. and Demaree, E. D., Influence of implantation of heavy metallic ions on the mechanical properties of two polymers, polystyrene and polyethylene terephthalate. *J. Mater. Res.*, 1997, **12**, 1917–1926.
15. Pivin, J. C., Contribution of ionizations and atomic displacements to the hardening of ion-irradiated polymers. *Thin Solid Films*, 1995, **263**, 185–193.
16. Ochsner, R., Klug, A., Zechel-Melonn, S., Gong, L. and Ryssel, H., Improvement of surface properties of polymers by ion implantation. *Nucl. Instrum. Meth. Phys. Res. B*, 1993, **80–81**, 1050–1054.
17. Yoshida, S., Ono, T., Shuichi, O. and Esashi, M., Reversible electrical modification on conductive polymer for proximity probe data storage. *Nanotechnology*, 2005, **16**, 2516–2520.

18. Wang, W. M., Wan, H. H., Rong, T. W., Bao, J. R. and Lin, S. H., Diode characteristics and degradation mechanism of ion implanted polyacetylene films. *Nucl. Instrum. Meth. Phys. Res. B*, 1991, **61**, 466–471.
19. Wang, W. M., Lin, S. H., Bao, J. R., Rong, T. W., Wan, H. H. and Sun, J., The *n*-type doping of polyaniline films by ion implantation. *Nucl. Instrum. Meth. Phys. Res. B*, 1993, **74**, 514–518.
20. Lin, S. H. *et al.*, Electrical properties of chemical-doped and ion-implanted polyacetylene films. *Nucl. Instrum. Meth. Phys. Res. B*, 1991, **59/60**, 1257–1262.
21. Hussain, A. M. P., Kumar, A., Singh, F. and Avasthi, D. K., Effects of 160 MeV Ni^{12+} ion irradiation on HCl doped polyaniline electrode. *J. Phys. D: Appl. Phys.*, 2006, **39**, 750–755.
22. Park, S. K., Lee, S. Y., Lee, C. S., Kim, H. M., Joo, J., Beag, Y. W. and Koh, S. K., High energy (MeV) ion-irradiated π-conjugated polyaniline: transition from insulating state to carbonized conducting state. *J. Appl. Phys.*, 2004, **96**, 1914–1918.
23. Tsukuda, S., Seki, S., Sugimoto, M. and Tagawa, S., Formation of nanowires based on π-conjugated polymers by high-energy ion beam irradiation. *Jpn. J. Appl. Phys.*, 2005, **44**, 5839–5842.
24. Tsukuda, S., Seki, S., Sugimoto, M., Tagawa, S., Idesaki, A., Tanaka, S. and Oshima, A., Fabrication of nanowires using high-energy ion beams. *J. Phys. Chem. B*, 2004, **108**, 3407–3409.
25. Srivastava, M. P., Mohanty, S. R., Annapoorni, S. and Rawat, R. S., Diode like behaviour of an ion irradiated polyaniline film. *Phys. Lett. A*, 1996, **215**, 63–68.
26. Venkatesan, T., High energy ion beam modification of polymer films. *Nucl. Instrum. Meth. Phys. Res. B*, 1984, **7–8**, 461–467.
27. Said, M. A., Balik, C. M. and Carlson, J. D., High-energy ion implantation of polymers: poly(vinylidene fluoride). *J. Polym. Sci. B: Polym. Phys.*, 1988, **26**, 1457–1467.
28. Kumar, R., De, U. and Prasad, R., Physical and chemical response of 70 MeV carbon ion irradiated polyether sulphone polymer. *Nucl. Instrum. Meth. Phys. Res. B*, 2006, **248**, 279–283.
29. Kumar, R., Prasad, R., Vijay, Y. K., Acharya, N. K., Verma, K. C. and De, U., Ion beam modification of CR-39 (DOP) and polyamide nylon-6 polymers. *Nucl. Instrum. Meth. Phys. Res. B*, 2003, **212**, 221–227.
30. Virk, H. S., Chandi, P. S. and Srivastava, A. K., Physical and chemical response of 70 MeV carbon ion irradiated Kapton-H polymer. *Bull. Mater. Sci.*, 2001, **24**, 529–534.
31. Virk, H. S., Chadi, P. S. and Srivastava, A. K., Electrical and optical response of lithium ion irradiated polyimide (kapton). *Radiat. Eff. Defects Solids*, 2001, **153**, 325–334.
32. Virk, H. S., Physical and chemical response of 70 MeV carbon ion irradiated Kapton-H polymer. *Nucl. Instrum. Meth. Phys. Res. B*, 2002, **191**, 739–743.
33. Zhu, Z., Liu, C., Sun, Y., Liu, J., Tang, Y., Jin, Y. and Du, J., Modification of polyethylene terephthalate under high-energy heavy ion irradiation. *Nucl. Instrum. Meth. Phys. Res. B*, 2002, **191**, 723–727.
34. Ram, M. K., Annapoorni, S. and Malhotra, B. D., Electrical properties of metal/Langmuir–Blodgett layer/semiconductive devices. *J. Appl. Polym. Sci.*, 1996, **60**, 407–411.
35. Pouget, J. P., Jozefowicz, M. E., Epstein, A. J., Tang, X. and MacDiarmid, A. G., X-ray structure of polyaniline. *Macromolecules*, 1991, **24**, 779–789.
36. Ziegler, J. F., SRIM-2003. *Nucl. Instrum. Meth. Phys. Res. B*, 2004, **219**, 1027–1036.
37. Alexander, L. E., *X-ray Diffraction Methods in Polymer Science*, Wiley, New York, 1969.
38. Hussain, A. M. P. and Kumar, A., Ion irradiation induced electrochemical stability enhancement of conducting polymer electrodes in supercapacitors. *Eur. Phys. J. Appl. Phys.*, 2006, **36**, 105–109.
39. Scrosati, B. (ed.), *Applications of Electroactive Polymers*, Chapman & Hall, London, 1993.
40. Hussain, A. M. P., Saikia, D., Singh, F., Avasthi, D. K. and Kumar, A., Effects of 160 MeV Ni^{12+} ion irradiation on polypyrrole conducting polymer electrode materials for all polymer redox supercapacitor. *Nucl. Instrum. Meth. Phys. Res. B*, 2005, **240**, 834–841.
41. Scherrer, P., *Gott. Nachr*, 1918, **2**, 98.
42. Singh, L. and Singh, R., Swift heavy ion induced modifications in polypropylene. *Nucl. Instrum. Meth. Phys. Res. B*, 2004, **225**, 478–482.
43. Kao, K. C. and Huang, W., *Electrical Transport in Solids: Organic Semiconductors*, Pergamon, Oxford, Great Britain, vol. 14, 1981.

ACKNOWLEDGEMENTS. We thank Inter University Accelerator Centre, New Delhi for providing beam time facility. We also thank Dr N. C. Mehra, University Science Instrumentation Centre, University of Delhi for his help in carrying out the SEM measurements.

Received 12 May 2009; revised accepted 14 October 2009

Formulation design of cyhalothrin pesticide microemulsion

Feng Zhao[1,*], Hong-ying Xia[2] and Jing-ling He[3]

[1]Jiangxi Key Laboratory of Organic Chemistry, Jiangxi Science and Technology Normal University, Nanchang 330013, China
[2]School of Chemistry Chemical Engineering, Jiangxi Science and Technology Normal University, Nanchang 330013, China
[3]Jiangxi Province Torch High Technology Development Corporation, Nanchang 330046, China

Microemulsion is regarded as the most promising pesticide formulation. However, the formulation of pesticide microemulsion is not easy and an efficient, scientific and inexpensive formulation design still remains elusive. Here, we present our formulation method based on the pseudo-ternary phase diagram and orthogonal design. In addition, the preparation of cyhalothrin microemulsion has been described and an explanation of the use of our approach is included.

Keywords: Cyhalothrin microemulsion, formula design, orthogonal design, pesticide formulations, pseudo-ternary phase diagram.

EMULSIFIABLE agricultural chemical formulations have been conveniently and widely used for a very long time[1]. However, emulsifiable solutions need large amounts of organic solvents such as toluene, dimethyl benzene, etc. which are harmful to man and his environment[2]. Hence, there is a demand for water-based, granular or control-release new pesticide formulations, which are clean and

*For correspondence. (e-mail: zhf19752003@yahoo.com.cn)